*bioRxiv version 1*

# A safer fluorescent *in situ* hybridization protocol for cryosections

Akane Chihara[1*], Rima Mizuno[1,2], Norie Kagawa[3], Ayuko Takayama[1], Akinori Okumura[1], Miyuki Suzuki[4], Yuki Shibata[5], Makoto Mochii[3], Hideyo Ohuchi[6], Keita Sato[6#], Ken-ichi T Suzuki[1,2#]

[1] Trans-Scale Biology Center, National Institute for Basic Biology, Okazaki, Aichi, 444-8585, Japan

[2] Department of Basic Biology, The Graduate University for Advanced Studies, SOKENDAI, Aichi, 444-8585, Japan

[3] Department of Life Science, Graduate School of Science, University of Hyogo, Ako-gun, Hyogo, 678-1297, Japan

[4] Division of Biology and Biological Engineering, California Institute of Technology, Pasadena, California, 91125, United States

[5] Department of Biology, Nippon Medical School, Musashino, Tokyo, 180-0023, Japan

[6] Department of Cytology and Histology, Faculty of Medicine, Dentistry, and Pharmaceutical Sciences, Okayama University, Okayama, 700-8558, Japan

[#] Correspondence to: suzuk107@nibb.ac.jp, keitasato@okayama-u.ac.jp

Running title: A safer FISH protocol for cryosections

# Abstract

Fluorescent *in situ* hybridization (FISH) enables highly sensitive, high-resolution detection of gene transcripts. Moreover, by employing multiple probes, this technique allows multiplexed, simultaneous detection of distinct gene expression patterns in a spatiotemporal manner, making it a valuable spatial transcriptomics approach. Owing to these advantages, FISH techniques are rapidly being adopted across diverse areas of basic biology. However, conventional protocols often rely on volatile, toxic reagents such as formalin or methanol, posing potential health risks to researchers. Here, we present a safer protocol that replaces these chemicals with low-toxicity and commercially available alternatives, without compromising the high detection sensitivity of FISH. We validated this protocol using both *in situ* hybridization chain reaction (HCR) and signal amplification by exchange reaction (SABER)-FISH in frozen sections of amphibians, *Pleurodeles waltl* and *Xenopus laevis*, as well as the teleost medaka (*Oryzias latipes*). Our results demonstrate successful multiplexed detection of various morphogenetic genes in these amphibian models and cell-type marker genes in the medaka using this safer protocol. The protocol has the additional advantage of requiring no proteolytic enzyme treatment. This protocol retains the benefits of high-sensitivity detection afforded by *in situ* HCR and SABER-FISH while providing a safer option for researchers, thereby offering a valuable tool for both basic biological and medical studies.



## Key words

*in situ* HCR, SABER-FISH, low-toxicity, cryosection, amphibians, medaka

# Introduction

mRNA *in situ* hybridization (ISH) has become a critical method for studying the distribution of mRNA in tissues, organs, and even whole bodies in various organisms. Initially, ISH employed probes labeled with radioactive isotopes such as $H^3$ and $S^{35}$, with detection achieved through autoradiography.[1–3] This was gradually superseded by a chromogenic detection method using probes labeled with biotin or digoxigenin to visualize target transcripts through enzymatic reactions using peroxidase or alkaline phosphatase.[4] More recently, fluorescence *in situ* hybridization (FISH) has emerged, enabling imaging through fluorophore-labeled probes using fluorescence microscopy.

A single-molecule transcript detection method, single-molecule FISH (smFISH), involves designing multiple specific-oligonucleotide probes complementary to particular target mRNAs, which hybridize to allow the detection of individual transcript molecules through fluorescence imaging.[5] However, simple increases in the number of probes alone are insufficient to achieve high sensitivity. To overcome this limitation, signal amplification techniques such as hybridization chain reaction (*in situ* HCR),[6,7] RNAScope,[8] and signal amplification by exchange reaction (SABER)-FISH[9] have been widely adopted in the improved smFISH. *In situ* HCR amplifies the secondary probe signal through isothermal amplification without enzymatic reactions, while methods such as RNAScope and SABER-FISH utilize branched secondary probes to hybridize multiple detection (imager) probes with fluorophores, significantly enhancing signal strength. These techniques enable the simultaneous detection of several mRNAs using distinct probes and allow multiplex FISH by repeated rounds of stripping and re-hybridization of probes to detect multiple sets of targets on the same section. Consequently, these approaches facilitate acquisition of the spatial transcriptomics involved in

underlying numerous gene expression patterns from the same tissue sections or fixed samples, making them highly versatile and powerful techniques.

Like other histological methods, FISH requires tissue or organ fixation, lipid removal, and enhanced probe permeability. Aldehyde-based fixatives such as formalin and organic solvents such as methanol are widely used for these purposes in basic biological experiments. However, these reagents pose significant risks due to their toxicity and volatility, requiring researchers to handle them with great care for experiment workers. Given these safety concerns, it has become increasingly important to develop safer laboratory environments and protocols to protect the health of researchers. To address these issues, this study aimed to develop a FISH protocol using low-toxicity fixatives and organic solvents as a safer alternative to hazardous reagents such as formalin and methanol. The protocol was evaluated and optimized through experimental applications in basic biology focusing specifically on *Xenopus laevis*, *Pleurodeles waltl*, and *Oryzias latipes.*

# Results

## *Establishment of a safer FISH protocol*

We developed a safer FISH protocol that does not rely on highly toxic chemicals and tested its suitability in various contexts in the investigations described below. The main features of our refined FISH protocol are as follows. First, when applied to amphibian or medaka tissue, the protocol permits fresh tissues or organs to be immediately embedded and frozen in OCT compound without any fixation step. This experimental step allows the protocol to be applied to spatial RNA-seq,[10,11] which also can omit the pre-fixation step, because lack of pre-fixation has no impact on the high quality mRNA sequences required for these spatial transcriptomics techniques. Similarly, pre-fixation was not necessarily required for FISH on the cryosections.

In our protocol, cryosections are post-fixed directly on the slide glasses after cryosectioning. Generally, 2–3% glutaraldehyde, 4% paraformaldehyde (4% PFA), and 3.7% formaldehyde (10% formalin) are used for tissue fixation; however, in this study, we examined two commercially available fixatives: ALTFiX and PAXgene®. The former is based on glyoxal, a dialdehyde compound, while the latter is ethanol-based and includes unspecified components. Both reagents are stated by their manufacturer to have low toxicity.

Secondly, our FISH protocol employs ethanol instead of methanol for the fixation, dehydration, delipidation, rehydration and permeabilization processes in order to minimize toxicity. The tissue integrity was well preserved with either ALTFiX or PAXgene®, and robust fluorescence signals were successfully detected in *in situ* HCR (as described below). Proteolytic enzymes such as proteinase K, trypsin, and pepsin have been widely used to enhance probe accessibility to target RNA in FISH so far; however, if not carefully optimized, they can damage tissues or adversely decrease the signal intensity of target mRNA. To circumvent this issue, our protocol does not include these proteolytic enzymes and instead uses a detergent solution containing Tween20 and sodium dodecyl sulfate (SDS) for a 30 min incubation at room temperature. This treatment effectively provided strong fluorescence signals without causing substantial tissue damage or target RNA degradation. Our workflow in developing a safer protocol is outlined in Figure 1.

### *Application of the safer protocol for detection of limb development-related genes in newts*

To evaluate the suitability of this safer protocol for detecting mRNA, we performed *in situ* HCR to visualize limb development–related gene expressions in the newt hindlimb bud. Using our protocol, we examined the expression patterns of *Fgf8* and *Fgf10* (Fig. 2A–D). These two

factors are known to form a positive feedback loop that maintains the stable outgrowth of the limb bud. Consistent with previous reports,[12-14] *Fgf8* expression was observed in the anterior region of the limb mesenchyme, whereas *Fgf10* expression was detected throughout the mesenchyme in a uniform manner. We also examined the expression patterns of *Hoxa11* and *Hoxa13*, two key genes involved in proximal–distal axis patterning in limb development (Fig. 2E–G). Generally, *Hoxa11* is associated with zeugopod formation, whereas *Hoxa13* is involved in vertebrate autopod development.[15,16] We also found that *Hoxa11* expression was distributed in the intermediate region of the newt hindlimb bud, whereas *Hoxa13* expression was localized to the distal region, consistent with a previous report.[17] Furthermore, we simultaneously detected both *Shh* and *Fgf8* signals in the same tissue section (Fig. 2H–J). In salamanders, *Shh*, which plays a crucial role in anterior–posterior (AP) axis specification in limb development, is expressed in the posterior mesenchyme, whereas *Fgf8* is expressed in the anterior mesenchyme.[12–14] Consistent with earlier reports, we observed that *Shh* transcripts were localized to the posterior mesenchyme, while the *Fgf8* signals appeared in the anterior mesenchyme in the newt hindlimb bud.

We further performed simultaneous triple-plex detection of *Hand2*, *Gli1*, and *Gli3* in the newt hindlimb bud. *Hand2* and *Gli1* are known to be expressed in the posterior mesenchyme under the control of *Shh* signaling, whereas *Gli3* is negatively regulated by *Shh* and is expressed in the anterior mesenchyme.[18,19] Therefore, these genes are generally employed for the readout of *Shh* signaling in limb development. Consistent with these previous reports, our results confirmed these expression patterns in the newt hindlimb (Fig. 3A–D). *Hand2* exhibited a relatively localized signal in the posterior region (Fig. 3A), whereas *Gli1* showed a gradient extending from the posterior toward the anterior region (Fig. 3B). In contrast, *Gli3* was detected in the anterior region opposite the *Shh*-expressing region, consistent with its negative regulation by *Shh* (Fig. 3C, D). Even when using the triple-plex fluorophores Alexa

Fluor 488, Alexa Fluor 514, and Alexa Fluor 546, which have close excitation wavelengths, the *in situ* HCR images clearly delineated the three distinct gene expression domains and no significant fluorescence bleed-through was observed.

### *Application of the safer protocol for in situ HCR in frogs*

We next tested this protocol in a model amphibian, *X. laevi*s, examining limb buds and adult leg joints. In previous reports, *Shh* is localized to the posterior mesenchyme, whereas *Fgf8* is found in the apical ectodermal ridge (AER) in *X. laevis*.[20,21] As anticipated, *Shh* and *Fgf8* mRNAs were simultaneously detected in the tadpole limb buds (Fig. 4A, B). In developing *X. laevis* hindlimbs, *Hoxa13* is expressed in the autopod region, while *Msx1* is localized more distally, directly beneath the AER. Consistent with earlier studies,[22,23] *in situ* HCR confirmed that *Msx1* was expressed in the distal region of the hindlimb bud, whereas *Hoxa13* appeared in the broader presumptive autopod region (Fig. 4C, D). Finally, *in situ* HCR with our protocol showed that the cartilage marker *Acan* (Aggrecan) and the joint marker *Prg4* (Proteoglycan4)[24,25], these mRNAs were specifically visualized in adult forelimb elbow joints (Fig. 4E).

### *Application of the safer protocol to the SABER-FISH method in amphibians*

In addition to demonstrating the utility of our safer FISH protocol in newts and frogs, we also examined its applicability to the SABER-FISH method. A key feature of SABER-FISH is "branching," in which branched secondary probes hybridize multiple fluorophore-labeled detection probes, thereby greatly enhancing signal intensity. In this study, we performed one round of branching for all SABER-FISH experiments to detect mRNA signals. First, to compare signals obtained with and without branching, we examined *Shh* expression in the newt larval brain using both *in situ* HCR and SABER-FISH. As expected, the *Shh* signal was clearly detected in the floor plate with both SABER-FISH and *in situ* HCR (Fig. 5A, B). We then

investigated the expression patterns of *Prrx1* and *Sox9* in frog hindlimb buds. During *Xenopus* limb development, *Prrx1* is broadly expressed in the limb mesenchyme, whereas *Sox9* is exclusively expressed in aggregating chondrocytes.[26,27] As expected, SABER-FISH also confirmed the specific expression patterns of each gene in the amphibian developing hindlimbs (Fig. 5C, D).

### *Application of the safer protocol to SABER-FISH mRNA detection in pre-fixed frozen sections of medaka retinas*

Next, to demonstrate the broader applicability of safer fixatives across different protocols and specimens, we examined SABER-FISH mRNA detection using a pre-fixed frozen section preparation protocol in the medaka retina. In this experiment, 4% PFA in a routine pre-fixation protocol for medaka retina was simply replaced with ALTFiX. Retinal cell-type-specific marker genes were visualized, including *gja10b* for horizontal cells and *cabp5a* for bipolar cells (Fig. 6).[28,29] In ALTFiX-fixed retinas, *gja10b* was detected in the boundary of the outer plexiform layer and the inner nuclear layer (INL), and *cabp5a* was detected in the outer part of the INL, as expected (Fig. 6). It should be noted that autofluorescence from photoreceptor inner segments was easily distinguished from punctate FISH signals. This result shows that a pre-fixed frozen section preparation protocol using a safer fixative is compatible with SABER-FISH in the medaka retina. Importantly, no special modifications were needed when exchanging the toxic 4% PFA for the safer ALTFiX in the medaka tissue preparation protocol.

## Discussion

mRNA FISH has been an essential research strategy in current biology, enabling the analysis of tissues, organs, and even whole organisms at single-cell resolution while simultaneously permitting examination of the expression of a limited set of genes in the same sample. *In situ* HCR, RNAScope, and SABER-FISH, each of which employs various amplification techniques, have been widely applied in most biological laboratories.[7–9] The simultaneous analysis of 2–4 genes in a single observation, although limited by the combination of fluorophores and their filters, is becoming increasingly routine. Given these developments, improved FISH protocols are expected to continue to grow in importance as research tools. The low-toxicity FISH protocol developed in this study offers a beneficial option for safeguarding the health of researchers performing routine experiments.

Glutaraldehyde and paraformaldehyde (formalin) are among the most widely used fixatives in various histological techniques, including FISH, due to their effectiveness in preserving tissue. However, their high toxicity and volatility necessitate careful handling to ensure the safety of researchers. To address this issue, we developed a safer protocol by replacing a toxic fixative with less toxic alternatives. One major concern when switching to alternative fixatives was the potential reduction in detection sensitivity for *in situ* HCR and SABER-FISH. Nonetheless, our protocol successfully detected the expression of even low-abundance transcripts in tissue sections, which are typically difficult to identify using RNA-Seq analysis. Despite being an aldehyde-based compound, glyoxal is a relatively low-toxicity and robust cross-linking fixative that has recently gained attention in the fields of life sciences.[30,31] Glyoxal not only serves as an effective substitute for formaldehyde (formalin) in mRNA FISH,[32] but it has also been reported to enhance signal sensitivity in certain cases.[33] Moreover, excessive fixation with strong cross-linking agents such as formalin often causes

signal attenuation in ISH. To mitigate this issue, tissues fixed with formalin generally require additional steps to partially reverse cross-linking, thereby improving probe accessibility to mRNA. These additional steps commonly involve proteolytic enzymes such as proteinase K or pepsin, which are widely employed in ISH. However, enzymatic treatments damage tissues and require careful optimization of parameters such as treatment time, concentration, and temperature, depending on the sample and the individual target genes. In contrast, our protocol using safer fixatives eliminates the need for proteolytic treatment using enzymes such as proteinase K, pepsin, and trypsin. By avoiding enzymatic digestion, the protocol not only simplifies the experimental workflow but also provides the additional advantage of better preservation of tissue morphology. Methanol is a highly toxic organic solvent that poses significant health risks in the laboratory. Nevertheless, conventional FISH protocols require methanol treatment for fixation, permeabilization, delipidation, and dehydration, because methanol effectively increases the probe penetration and enhances the signals. Indeed, in zebrafish whole-mount FISH, methanol treatment is critical.[34] On the other hand, because it uses glyoxal-based fixation, our protocol does not require methanol treatment.

In this study, we evaluated the application of our low-toxicity protocol to both *in situ* HCR and SABER-FISH using frozen amphibian tissue sections as a model experiment. *In situ* HCR is a user-friendly method because the design and synthesis of the probes (initiator probe and amplifier) can be outsourced to suppliers or designed independently by researchers, enabling us to readily perform this technique. In the amphibians *X. laevis*, *A. mexicanum*, and *P. waltl*, *in situ* HCR technology enables the detection of mRNA expression with high sensitivity and resolution.[12,13,35–37] Moreover, an improved version of *in situ* HCR that enhances probe permeability by using shortened hairpin amplifier probes was recently reported.[38] Integrating this improved *in situ* HCR with our protocol could not only enhance stability but also improve the consistency and reliability of signal detection, thereby increasing the success

rate of experiments. On the other hand, SABER-FISH is somewhat less user-friendly, as it requires researchers to design and synthesize probes themselves by using *in vitro* primer exchange reactions (PER).[39] Nevertheless, the PER concatemers, branch probes, and fluorescent imager probes can be used following the procedures described in the original publication[39], and the required oligos can be synthesized by ordering sequences from a supplier. One key advantage of SABER-FISH is that the use of branch probes allows an increase in the number of hybridized fluorescent imager probes. This can amplify signals and enable the detection of low-abundance mRNAs that are challenging to identify with *in situ* HCR. However, when we designed probes for the same gene ORF and used them to compare their performance of *in situ* HCR and SABER-FISH, we observed some cases where only one method successfully detected the target. Although the exact reason for this differential efficacy remains unknown, it is possible that the position or number of probes designed by each method affects the efficiency of hybridization against certain target mRNAs.

## Limitations of the study

Certain limitations of our low-toxicity FISH protocol bear mention. First, the protocol has not yet been validated for use with whole-mount or paraffin-embedded samples in vertebrates, and further investigation of these applications is warranted. Nevertheless, glyoxal-based fixation has proven effective in whole mount FISH of *Drosophila* embryos[32], suggesting that it may also be applicable to vertebrate embryos and tissues. Second, particularly for soft and fragile material such as embryos, it may be preferable to fix the samples before embedding them. Third, despite the fact that we observed virtually no loss of FISH signal sensitivity in our experiments, glyoxal-based fixation is slightly less effective at preserving cellular and tissue morphology, nuclear structure in particular, compared to paraformaldehyde or other aldehyde fixatives. Thus, the advantages and disadvantages are essentially a trade-off: the modest compromise in

morphology is offset by the ability to advance research while markedly reducing researcher exposure to toxic formalin and methanol. Fourth, there is still a safety concern remaining about the continued use of formamide, an organic solvent widely employed to facilitate probe hybridization to target genomic DNA and RNA in the conventional FISH protocols. High concentrations of formamide can also pose health risks to researchers and lab staff conducting experiments. Consequently, several ISH protocols that utilize alternative organic solvents or reagents such as urea and ethylene carbonate have been described.[40,41] Notably, ethylene carbonate both promotes hybridization and shortens hybridization times in *in situ* HCR.[42] In the future, we will incorporate this reagent into our FISH protocol to further improve its safety and ease of use in the laboratory.

## Materials and Methods

### *Animals*

Iberian ribbed newts (*Pleurodeles waltl*) were provided by the National Bioresource Project, Amphibian Research Center, Hiroshima University. African clawed frog (*Xenopus laevis*) tadpoles and adults were purchased from suppliers. Medaka (*Oryzias latipes*) strain d-rR was maintained and bred at Okayama University. For anesthesia before the sample collection of amphibians, MS-222 (Sigma, St. Louis, MO, USA) was used at a final concentration of 0.02%. For euthanasia of medaka, 0.1% (v/v) of 2-phenoxyethanol was used. Developmental stages were determined according to the *P. walt*l and *X. laevis* staging.[43,44] Tissues were collected from embryos and larvae (st. 40 to st. 43 for newt limb bud and brain, st. 51 to st. 54 for frog limb bud) and frog under deep anesthesia and euthanasia. All animal care was approved by the

Institutional Animal Care and Use Committee of the National Institutes of Natural Sciences, University of Hyogo, and Okayama University.

### *Preparation of cryosections*

Tissues were embedded in Tissue-Tek O.C.T compound (SAKURA, Nagano, Japan) and then immediately frozen on an aluminum plate with liquid nitrogen. The embedded tissues were sectioned at 14 μm using a Cryostar NX70 (Thermofisher, USA) and mounted on MAS-coated glass slides (Matsunami Glass, Osaka, Japan). The mounted sections were then fixed using either of two formaldehyde-free tissue fixatives, ALTFiX (FALMA, Tokyo, Japan) or PAXgene® (Qiagen, Hilden, Germany), at room temperature for 30 min and dehydrated with a graded ethanol series (50%, 70%, 100%, 100%). After air-drying for 30 min, the slides were bordered with an ImmEdge Hydrophobic Barrier PAP Pen (Vector Laboratories, CA, USA). The sections were immersed in a modified detergent solution[45] (Table S1) for 30 min at room temperature and then washed twice with Phosphate Buffered Saline (PBS). For the medaka retina samples, tissues were sectioned after pre-fixation. Following dissection, the tissues were fixed overnight in ALTFiX at 4°C. The samples were then immersed in 20% sucrose in PBS overnight for cryoprotection and subsequently embedded in OCT compound and frozen in a deep freezer at −80°C. Frozen medaka retinas were sectioned at a thickness of 15 μm using a cryostat (Polar; Sakura Finetek, Tokyo, Japan) and mounted on CREST-coated glass slides (Matsunami Glass, Osaka, Japan).

### *Sequences for probe design*

For the probe design in SABER-FISH in this study, all coding sequences of target genes were retrieved from Xenbase, two *P. waltl* genome projects, and the NCBI nucleotide database.[46,47]

### *Hybridization chain reaction (in situ HCR)*

Next, the samples were pre-hybridized with a probe-hybridization buffer for 10 min at 37 °C. HCR probes were purchased from Molecular Instruments (CA, USA). Probe solution (100 µl of probe-hybridization buffer containing 0.4 µl of 1 µM each initiator probe) was applied, and the samples were incubated overnight at 37 °C. The next day, the samples were washed in decreasing concentrations of probe-wash buffer/5x sodium chloride sodium citrate and 0.1% Tween20 (SSCT), followed by a final wash in 100% 5x SSCT for 15 min at 37°C. Then, the slides were again washed for 15 min in 100% 5x SSCT. The samples were incubated with an amplification buffer at room temperature for 30 min. After denaturation of hairpin probes at 95 °C, 100 µl of hairpin solution (2 µl each of 3 µM hairpin1 and 2 probes and 100 µl of amplification buffer) were applied, and the samples were incubated overnight at room temperature in the dark. The following day, the amplified samples were washed twice for 30 min and once for 5 min in 5x SSCT at room temperature. Finally, the slides were covered with a mounting medium (ProLong™ Gold Antifade Mountant with DNA Stain DAPI, Thermo Fisher Scientific, USA) and cover glasses.

### *Signal Amplification By Exchange Reaction (SABER)-FISH*

Probes for *Prrx1* and *Sox9* of *X. laevis*, *Shh* of *P.waltl*, and *gja10b* and *cabp5a* of medaka were designed by running the blockParse script from OligoMiner package on their coding sequences.[48] Primer exchange reactions were performed following the previous reports.[9,49] Fluorescent signals were amplified and detected with one branching round as follows. Sections were treated with the detergent solution at room temperature, followed by three times rinses in

PBS containing 0.1 % Tween20 (PBST). They were pre-hybridized in Prehyb (40% formamide, 2× SSC, 1% Tween20, 1× Denhardt's solution, 100 μg/mL heparin sodium, and 0.5 μM random 20 mer oligo DNA) at 43°C for 10 min, then incubated with the respective probes at 1 μg/mL in Hyb1.1 (Prehyb containing 10% dextran sulfate (FUJIFILM Wako Pure Chemical Corporation 197-09984)) at 43°C for 16 h. Post-hybridization washes were performed in Whyb (40% formamide, 2× SSC, 1% Tween20) and 2× SSCT. For signal amplification, branch oligos (1 μg/mL in Hyb1.1) were applied for 6–12 h at 37°C, followed by SSCT washes. Fluorophore-conjugated oligos (0.1 μM) diluted in Hyb2.1 (0.1% Tween20, 1× Denhardt's solution, 100 μg/mL heparin sodium, and 0.5 μM random 20 mer oligo DNA in PBS) were added for 1 h at 37°C. Finally, the sections were counterstained with DAPI (0.2 μg/mL), rinsed in PBST, and coverslipped with homemade polyvinyl alcohol/glycerol mounting medium. The oligonucleotide sequences for SABER-FISH probes are described in Table S2.

### *Imaging and analysis*

For acquisition of images for triple-plex visualization of SHH-pathway transcripts, STELLARIS 8 (Leica Microsystems GmbH, Wetzlar, Germany) was used. All other samples were observed under a confocal microscope Nikon A1R (Nikon, Tokyo, Japan). All images were visualized using Fiji software,[50] with contrast adjusted uniformly across all samples.

## Acknowledgments

*P. waltl* newts were provided by the Hiroshima University Amphibian Research Center, and the National BioResource Project of MEXT. This research was supported by the following funding sources: JST, CREST Grant Number JPMJCR2025 to K.T.S. and JSPS KAKENHI Grant Numbers 21H03829 to K.T.S. and 23K05850 to K.S.; the NIBB Collaborative Research Program (24NIBB328) to M.M.; Joint Research of the Exploratory Research Center on Life

and Living Systems (ExCELLS) Grant Numbers 23-S6 and 22-S3 to K.T.S.; and a grant from the Japan Foundation for Applied Enzymology to K.S. Confocal images were acquired at the Optics and Imaging Facility of the NIBB Trans-Scale Biology Center.

## Contributions

Conceptualization: KTS

Methodology: KS, KTS

Experiments: AC, RM, NK, AT, AO, MS, YS, KS, KTS

Visualization: AC, RM, NK, KS, KTS

Funding acquisition: KS, KTS

Project administration: KS, KTS

Supervision: MM, HO

Writing – original draft: AC, RM, KS, KTS

Writing – review & editing: All authors

# References


1. Gall JG, Pardue ML. Formation and detection of RNA-DNA hybrid molecules in cytological preparations. *Proc Natl Acad Sci U S A*. 1969;63(2):378-383. https://doi.org/10.1073/pnas.63.2.378

2. Singer RH, Ward DC. Actin gene expression visualized in chicken muscle tissue culture by using in situ hybridization with a biotinated nucleotide analog. *Proc Natl Acad Sci U S A*. 1982;79(23):7331-7335. https://doi.org/10.1073/pnas.79.23.7331

3. Cox KH, DeLeon DV, Angerer LM, Angerer RC. Detection of mrnas in sea urchin embryos by in situ hybridization using asymmetric RNA probes. *Dev Biol*. 1984;101(2):485-502. https://doi.org/10.1016/0012-1606(84)90162-3

4. Tautz D, Pfeifle C. A non-radioactive in situ hybridization method for the localization of specific RNAs in Drosophila embryos reveals translational control of the segmentation gene hunchback. *Chromosoma*. 1989;98(2):81-85. https://doi.org/10.1007/bf00291041

5. Raj A, van den Bogaard P, Rifkin SA, van Oudenaarden A, Tyagi S. Imaging individual mRNA molecules using multiple singly labeled probes. *Nat Methods*. 2008;5(10):877-879. https://doi.org/10.1038/nmeth.1253

6. Choi HMT, Chang JY, Trinh LA, Padilla JE, Fraser SE, Pierce NA. Programmable in situ amplification for multiplexed imaging of mRNA expression. *Nat Biotechnol*. 2010;28(11):1208-1212. https://doi.org/10.1038/nbt.1692

7. Choi HMT, Schwarzkopf M, Fornace ME, et al. Third-generation in situ hybridization chain reaction: multiplexed, quantitative, sensitive, versatile, robust. *Development*. 2018;145(12):dev165753. https://doi.org/10.1242/dev.165753

8. Wang F, Flanagan J, Su N, et al. RNAscope: a novel in situ RNA analysis platform for formalin-fixed, paraffin-embedded tissues. *J Mol Diagn*. 2012;14(1):22-29. https://doi.org/10.1016/j.jmoldx.2011.08.002

9. Kishi JY, Lapan SW, Beliveau BJ, et al. SABER amplifies FISH: enhanced multiplexed imaging of RNA and DNA in cells and tissues. *Nat Methods*. 2019;16(6):533-544. https://doi.org/10.1038/s41592-019-0404-0

10. Ståhl PL, Salmén F, Vickovic S, et al. Visualization and analysis of gene expression in tissue sections by spatial transcriptomics. *Science*. 2016;353(6294):78-82. https://doi.org/10.1126/science.aaf2403

11. Chen A, Liao S, Cheng M, et al. Spatiotemporal transcriptomic atlas of mouse organogenesis using DNA nanoball-patterned arrays. *Cell*. 2022;185(10):1777-1792.e21. https://doi.org/10.1016/j.cell.2022.04.003

12. Glotzer GL, Tardivo P, Tanaka EM. Canonical Wnt signaling and the regulation of

divergent mesenchymal Fgf8 expression in axolotl limb development and regeneration. *Elife*. 2022;11. https://doi.org/10.7554/eLife.79762

13. Lovely AM, Duerr TJ, Qiu Q, Galvan S, Voss SR, Monaghan JR. Wnt signaling coordinates the expression of limb patterning genes during axolotl forelimb development and regeneration. *Front Cell Dev Biol*. 2022;10:814250. https://doi.org/10.3389/fcell.2022.814250

14. Suzuki M, Okumura A, Chihara A, et al. Fgf10 mutant newts regenerate normal hindlimbs despite severe developmental defects. *Proc Natl Acad Sci U S A*. 2024;121(11):e2314911121. https://doi.org/10.1073/pnas.2314911121

15. Davis AP, Witte DP, Hsieh-Li HM, Potter SS, Capecchi MR. Absence of radius and ulna in mice lacking hoxa-11 and hoxd-11. *Nature*. 1995;375(6534):791-795. https://doi.org/10.1038/375791a0

16. Fromental-Ramain C, Warot X, Messadecq N, LeMeur M, Dollé P, Chambon P. Hoxa-13 and Hoxd-13 play a crucial role in the patterning of the limb autopod. *Development*. 1996;122(10):2997-3011. https://doi.org/10.1242/dev.122.10.2997

17. Takeuchi T, Matsubara H, Minamitani F, et al. Newt Hoxa13 has an essential and predominant role in digit formation during development and regeneration. *Development*. 2022;149(5):dev200282. https://doi.org/10.1242/dev.200282

18. Ahn S, Joyner AL. Dynamic changes in the response of cells to positive hedgehog signaling during mouse limb patterning. *Cell*. 2004;118(4):505-516. https://doi.org/10.1016/j.cell.2004.07.023

19. Galli A, Robay D, Osterwalder M, et al. Distinct roles of Hand2 in initiating polarity and posterior Shh expression during the onset of mouse limb bud development. *PLoS Genet*. 2010;6(4):e1000901. https://doi.org/10.1371/journal.pgen.1000901

20. Endo T, Yokoyama H, Tamura K, Ide H. Shh expression in developing and regenerating limb buds of Xenopus laevis. *Dev Dyn*. 1997;209(2):227-232. https://doi.org/10.1002/(SICI)1097-0177(199706)209:2<227::AID-AJA8>3.0.CO;2-K

21. Christen B, Slack JM. FGF-8 is associated with anteroposterior patterning and limb regeneration in Xenopus. *Dev Biol*. 1997;192(2):455-466. https://doi.org/10.1006/dbio.1997.8732

22. Endo T, Tamura K, Ide H. Analysis of gene expressions during Xenopus forelimb regeneration. *Dev Biol*. 2000;220(2):296-306. https://doi.org/10.1006/dbio.2000.9641

23. Barker DM, Beck CW. Overexpression of the transcription factor Msx1 is insufficient to drive complete regeneration of refractory stage Xenopus laevis hindlimbs. *Dev Dyn*. 2009;238(6):1366-1378. https://doi.org/10.1002/dvdy.21923

24. Watanabe H, Kimata K, Line S, et al. Mouse cartilage matrix deficiency (cmd) caused by a 7 bp deletion in the aggrecan gene. *Nat Genet*. 1994;7(2):154-157. https://doi.org/10.1038/ng0694-154

25. Rhee DK, Marcelino J, Baker M, et al. The secreted glycoprotein lubricin protects

cartilage surfaces and inhibits synovial cell overgrowth. *J Clin Invest*. 2005;115(3):622-631. https://doi.org/10.1172/JCI22263

26. Suzuki M, Satoh A, Ide H, Tamura K. Transgenic Xenopus with prx1 limb enhancer reveals crucial contribution of MEK/ERK and PI3K/AKT pathways in blastema formation during limb regeneration. *Dev Biol*. 2007;304(2):675-686. https://doi.org/10.1016/j.ydbio.2007.01.019

27. Satoh A, Endo T, Abe M, et al. Characterization of Xenopus digits and regenerated limbs of the froglet. *Dev Dyn*. 2006;235(12):3316-3326. https://doi.org/10.1002/dvdy.20985

28. Klaassen LJ, de Graaff W, van Asselt JB, Klooster J, Kamermans M. Specific connectivity between photoreceptors and horizontal cells in the zebrafish retina. *J Neurophysiol*. 2016;116(6):2799-2814. https://doi.org/10.1152/jn.00449.2016

29. Glasauer S, Neuhauss S. Expression of CaBP transcripts in retinal bipolar cells of developing and adult zebrafish. *Matters*. Published online April 21, 2016. https://doi.org/10.19185/matters.201604000009

30. Richter KN, Revelo NH, Seitz KJ, et al. Glyoxal as an alternative fixative to formaldehyde in immunostaining and super-resolution microscopy. *EMBO J*. 2018;37(1):139-159. https://doi.org/10.15252/embj.201695709

31. Konno K, Yamasaki M, Miyazaki T, Watanabe M. Glyoxal fixation: An approach to solve immunohistochemical problem in neuroscience research. *Sci Adv*. 2023;9(28):eadf7084. https://doi.org/10.1126/sciadv.adf7084

32. Amin S, Basu M, Buzinova V, et al. Glyoxal-based fixation of Drosophila embryos for immunofluorescence staining and RNA in situ hybridization. *STAR Protoc*. 2023;4(3):102385. https://doi.org/10.1016/j.xpro.2023.102385

33. Yao RW, Luan PF, Chen LL. An optimized fixation method containing glyoxal and paraformaldehyde for imaging nuclear bodies. *RNA*. 2021;27(6):725-733. https://doi.org/10.1261/rna.078671.120

34. Oka Y, Sato TN. Whole-mount single molecule FISH method for zebrafish embryo. *Sci Rep*. 2015;5(1):8571. https://doi.org/10.1038/srep08571

35. Aztekin C, Hiscock TW, Gurdon J, Jullien J, Marioni J, Simons BD. Secreted inhibitors drive the loss of regeneration competence in Xenopus limbs. *Development*. 2021;148(11). https://doi.org/10.1242/dev.199158

36. Lee J, Møller AF, Chae S, et al. A single-cell, time-resolved profiling of Xenopus mucociliary epithelium reveals nonhierarchical model of development. *Sci Adv*. 2023;9(14):eadd5745. https://doi.org/10.1126/sciadv.add5745

37. Jaeger ECB, Vijatovic D, Deryckere A, et al. Adeno-associated viral tools to trace neural development and connectivity across amphibians. *Dev Cell*. 2025;60(5):794-812.e6. https://doi.org/10.1016/j.devcel.2024.10.025

38. Tsuneoka Y, Funato H. Modified in situ hybridization chain reaction using short hairpin

DNAs. *Front Mol Neurosci*. 2020;13:75. https://doi.org/10.3389/fnmol.2020.00075

39. Kishi JY, Schaus TE, Gopalkrishnan N, Xuan F, Yin P. Programmable autonomous synthesis of single-stranded DNA. *Nat Chem*. 2018;10(2):155-164. https://doi.org/10.1038/nchem.2872

40. Matthiesen SH, Hansen CM. Fast and non-toxic in situ hybridization without blocking of repetitive sequences. *PLoS One*. 2012;7(7):e40675. https://doi.org/10.1371/journal.pone.0040675

41. Sinigaglia C, Thiel D, Hejnol A, Houliston E, Leclère L. A safer, urea-based in situ hybridization method improves detection of gene expression in diverse animal species. *Dev Biol*. 2018;434(1):15-23. https://doi.org/10.1016/j.ydbio.2017.11.015

42. Mikami K, Kaneko M, Kimoto T. Doping-dependent fixed charges in $SiC/SiO_2$ structure. *Appl Phys Express*. 2025;18(3):034002. https://doi.org/10.35848/1882-0786/adb539

43. Shi DL, Boucaut JC. The chronological development of the urodele amphibian Pleurodeles waltl (Michah). *Int J Dev Biol*. 1995;39(3):427-441. https://pubmed.ncbi.nlm.nih.gov/7577434/

44. Nieuwkoop PD (pieter D, Faber J. Normal table of Xenopus laevis (Daudin) : a systematical and chronological survey of the development from the fertilized egg till the end of metamorphosis. Published online 1994. Accessed May 20, 2025. https://ci.nii.ac.jp/ncid/BA28324104

45. Morabito A, Malkmus J, Pancho A, Zuniga A, Zeller R, Sheth R. Optimized protocol for whole-mount RNA fluorescent in situ hybridization using oxidation-mediated autofluorescence reduction on mouse embryos. *STAR Protoc*. 2023;4(4):102603. https://doi.org/10.1016/j.xpro.2023.102603

46. Fisher M, James-Zorn C, Ponferrada V, et al. Xenbase: key features and resources of the Xenopus model organism knowledgebase. *Genetics*. 2023;224(1):iyad018. https://doi.org/10.1093/genetics/iyad018

47. Brown T, Mishra K, Elewa A, et al. Chromosome-scale genome assembly reveals how repeat elements shape non-coding RNA landscapes active during newt limb regeneration. *Cell Genom*. 2025;5(2):100761. https://doi.org/10.1016/j.xgen.2025.100761

48. Beliveau BJ, Kishi JY, Nir G, et al. OligoMiner provides a rapid, flexible environment for the design of genome-scale oligonucleotide in situ hybridization probes. *Proc Natl Acad Sci U S A*. 2018;115(10):E2183-E2192. https://doi.org/10.1073/pnas.1714530115

49. Fukuda A, Sato K, Fujimori C, et al. Direct photoreception by pituitary endocrine cells regulates hormone release and pigmentation. *Science*. 2025;387(6729):43-48. https://doi.org/10.1126/science.adj9687

50. Schindelin J, Arganda-Carreras I, Frise E, et al. Fiji: an open-source platform for biological-image analysis. *Nat Methods*. 2012;9(7):676-682. https://doi.org/10.1038/nmeth.2019

## Figure legends

**Figure 1.** Workflow of a safer FISH protocol. Tissues or organs are sampled on Day 0, fixed when required, embedded in OCT, and then cryosectioned. At Day 1 our FISH protocol begins. Steps highlighted in green denote the novel modifications introduced in this study. Cryosections mounted on glass slides are fixed with a safer fixative, dehydrated and rehydrated through graded ethanol series, and then permeabilized with a detergent solution to enhance probe penetration. Subsequent steps follow the standard HCR- or SABER-FISH workflow.

**Figure 2.** mRNA detection of limb development-related genes by a safer *in situ* HCR protocol in newt hindlimb bud sections. *Fgf8* (A; red) is enriched in the anterior mesenchyme, whereas *Fgf10* (B; green) is detected sparsely throughout the bud; the merged image is shown in C. Nuclei is counterstained with DAPI (D). *Hoxa11* (E; green) and *Hoxa13* (F; magenta) exhibit complementary expression domains along the proximo-distal axis; the merged image is shown in G. *Shh* (H; green) and *Fgf8* (I; magenta) mRNAs are restricted to the posterior and anterior mesenchyme, respectively; the merged image is shown in J. Dotted lines indicate the epithelial–mesenchymal boundary. Sections in A–D and H-J were post-fixed with ALTFiX, whereas sections in E–G were fixed with PAXgene®. Abbreviations: A, Anterior; P, Posterior direction. Scale bar, 50 µm.

**Figure 3.** Triple-plexed visualization of SHH-pathway transcripts by a safer *in situ* HCR protocol in newt hindlimb bud sections. Sections were post-fixed with ALTFiX. (A–C) Pseudocolor images showing *Hand2* (green), *Gli1* (magenta), and *Gli3* (cyan) mRNAs, respectively; (D) merged view of all three channels. *Hand2* labels the posterior *Shh*-expressing domain, while *Gli1* and *Gli3* are positively and negatively regulated by SHH signaling, respectively, resulting in sharply segregated expression domains along the anterior–posterior

axis. Solid white lines outline the limb bud; dotted white lines indicate the epithelial–mesenchymal boundary. Abbreviations: A, Anterior; P, Posterior direction. Scale bar: 50 µm.

**Figure 4.** Representative images of *in situ* HCR performed using a safer protocol in frog tissue sections. Nuclei were counterstained with DAPI in A,C. (A,B) *Shh* (green) and *Fgf8* (magenta) mRNAs are restricted to the posterior hindlimb bud mesenchyme and AER, respectively. Scale bar: 100 µm. (A) Merged view of the three channels. (B) Enlarged view of the area outlined with a dashed line in A. (C,D) *Hoxa13* (green) and *Msx1* (magenta) exhibit complementary expression domains along the proximo–distal axis in the hindlimb bud. Dotted white lines indicate the epithelial–mesenchymal boundary. Scale bars: 200 µm. (C) Merged view of the three channels. (D) Enlarged view of the area outlined with a dashed line. (E) *Prg4* (green) and *Acan* (magenta) signals are observed in articular cartilage and chondrocytes, respectively, in the adult forelimb joint. The asterisk marks autofluorescence in the outer layer of epidermis. Abbreviations:R/U, Radius/Ulna; Hu, humerus. Scale bar: 100 µm. Sections in A, B, and E were post-fixed with PAXgene®, whereas sections in C and D were fixed with ALTFiX.

**Figure 5.** *In situ* mRNA detection using a safer SABER-FISH protocol in amphibians, with tissue sections post-fixed in ALTFiX. (A, B) *Shh* expression (green) in the *P. waltl* larval brain. Image A and B shows the result of *in situ* HCR and SABER-FISH, respectively. FP shows floor plate. Scale bars: 50 µm. (C, D) Simultaneous detection of *Prrx1* (green) and *Sox9* (magenta) in the *X. laevis* tadpole hindlimb buds, showing their expression in mesenchymal cells and chondrocytes. (C) *Prrx1* (green) and *Sox9* (magenta) expression along the dorsal–ventral axis at the stage 52. (D) *Prrx1* (green) and *Sox9* (magenta) expression along the anterior–posterior axis at the stage 54. Abbreviations: D, Dorsal; V, Ventral; P, Proximal; Di, Distal; A, Anterior; Po, Posterior direction. Scale bars: 100 µm.

**Figure 6.** *In situ* mRNA detection using a safer SABER-FISH protocol in medaka retinas pre-fixed with ALTFiX. mRNA expressions of *cabp5a* (green, A) and *gja10b* (magenta, B) were detected in the medaka retina. A merged view is shown in C. Nuclei were counterstained with DAPI. The asterisk marks autofluorescence arising from the inner segments of photoreceptor cells. RPE, retinal pigment epithelium; ONL, outer nuclear layer; OPL, outer plexiform layer; INL, inner plexiform layer; IPL, inner plexiform layer; GCL, ganglion cell layer. Scale bars: 50 μm.

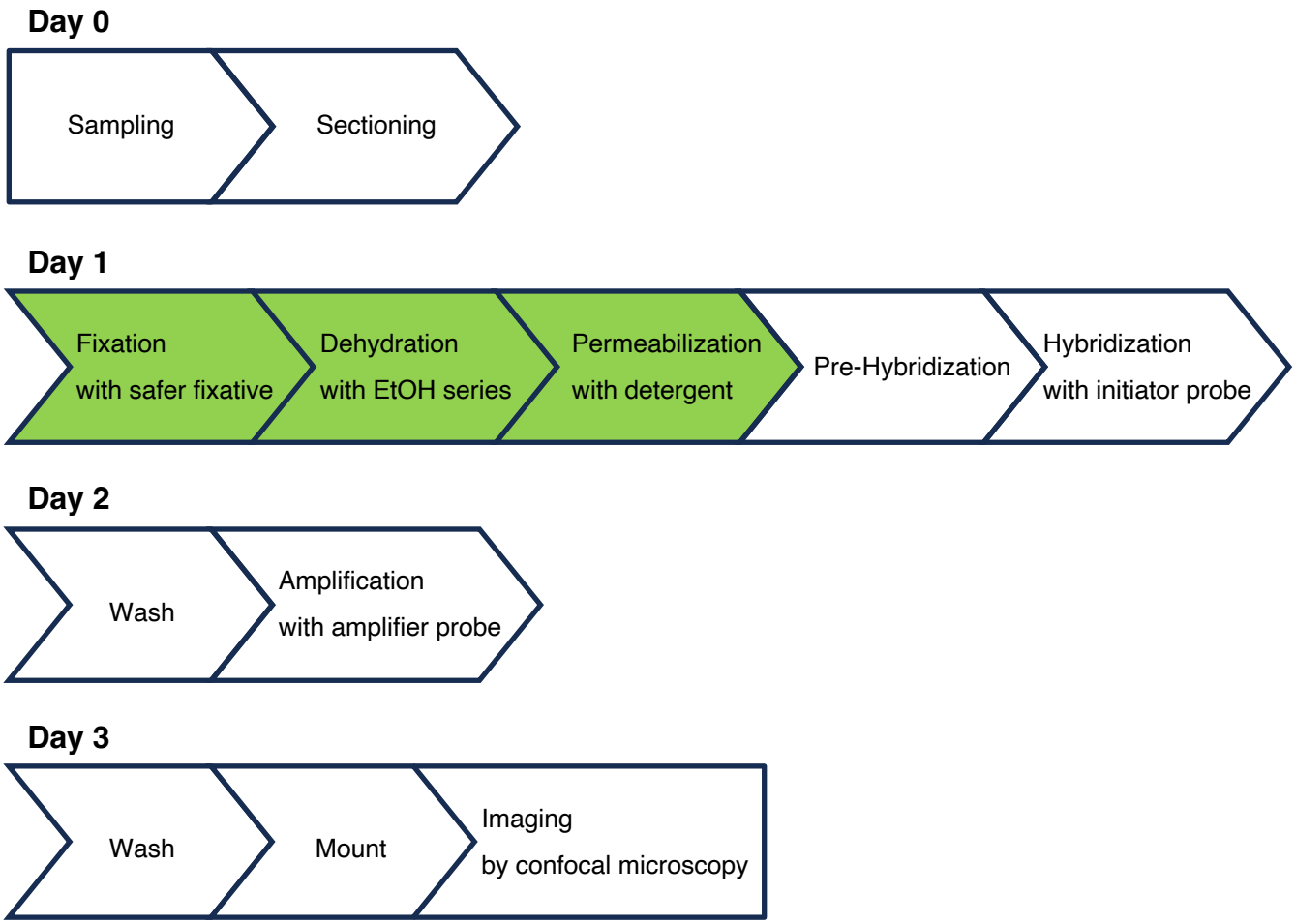
Day 0
Sampling
Sectioning
Day 1
Fixation
with safer fixative
Dehydration
with EtOH series
Permeabilization
with detergent
Pre-Hybridization
Hybridization
with initiator probe
Day 2
Wash
Amplification
with amplifier probe
Day 3
Wash
Mount
Imaging
by confocal microscopy

Fig.1

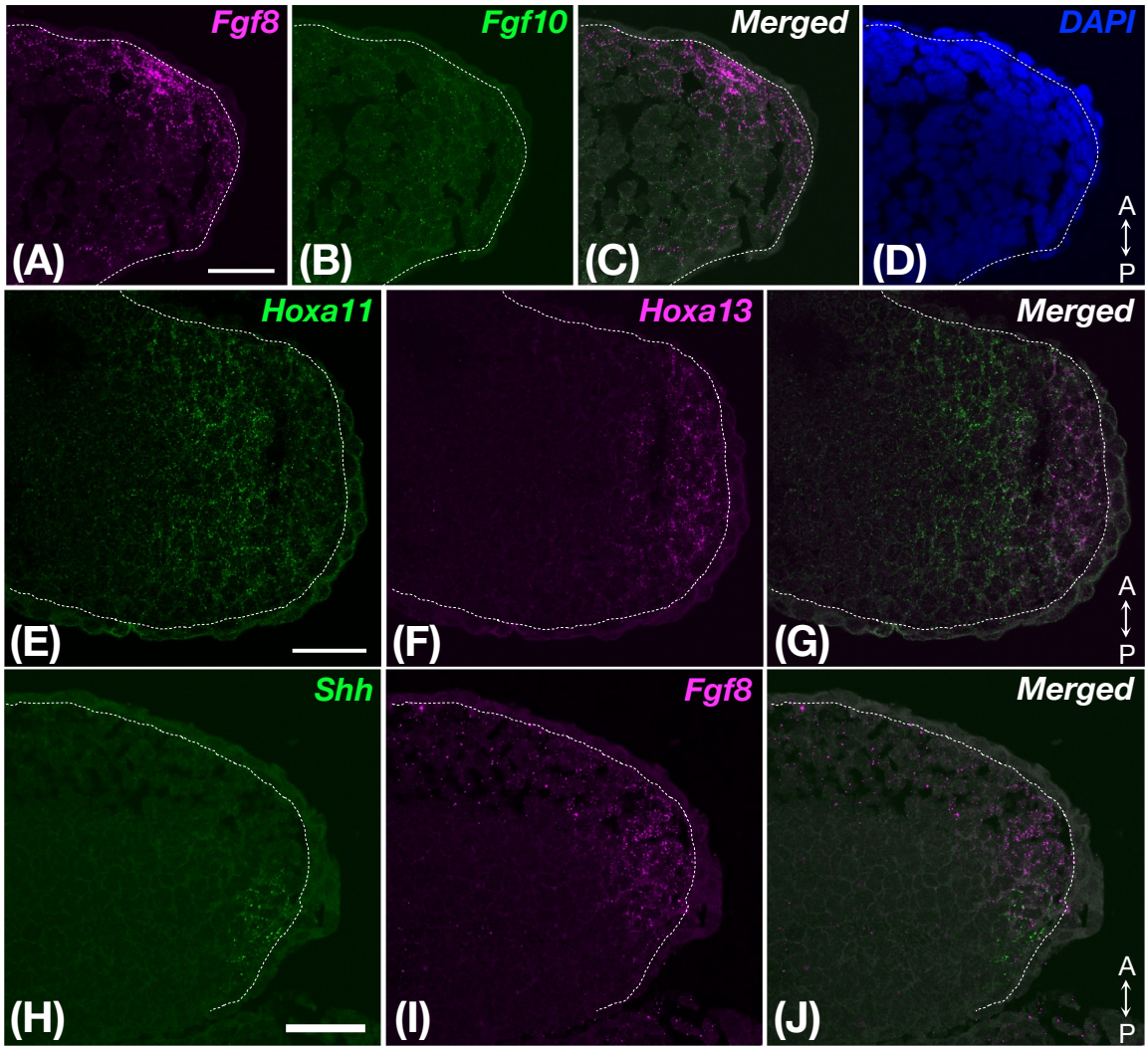
Fgf8
(A)
Fgf10
(B)
Merged
(C)
DAPI
(D)
A
P
Hoxa11
(E)
Hoxa13
(F)
Merged
(G)
A
P
Shh
(H)
Fgf8
(I)
Merged
(J)
A
P

Fig.2

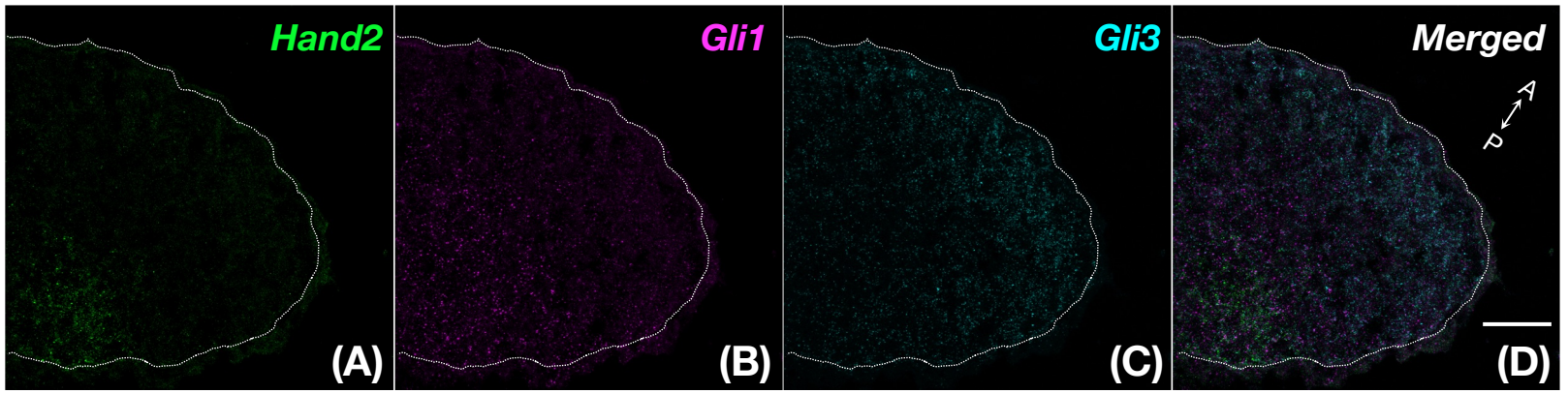


Fig.3

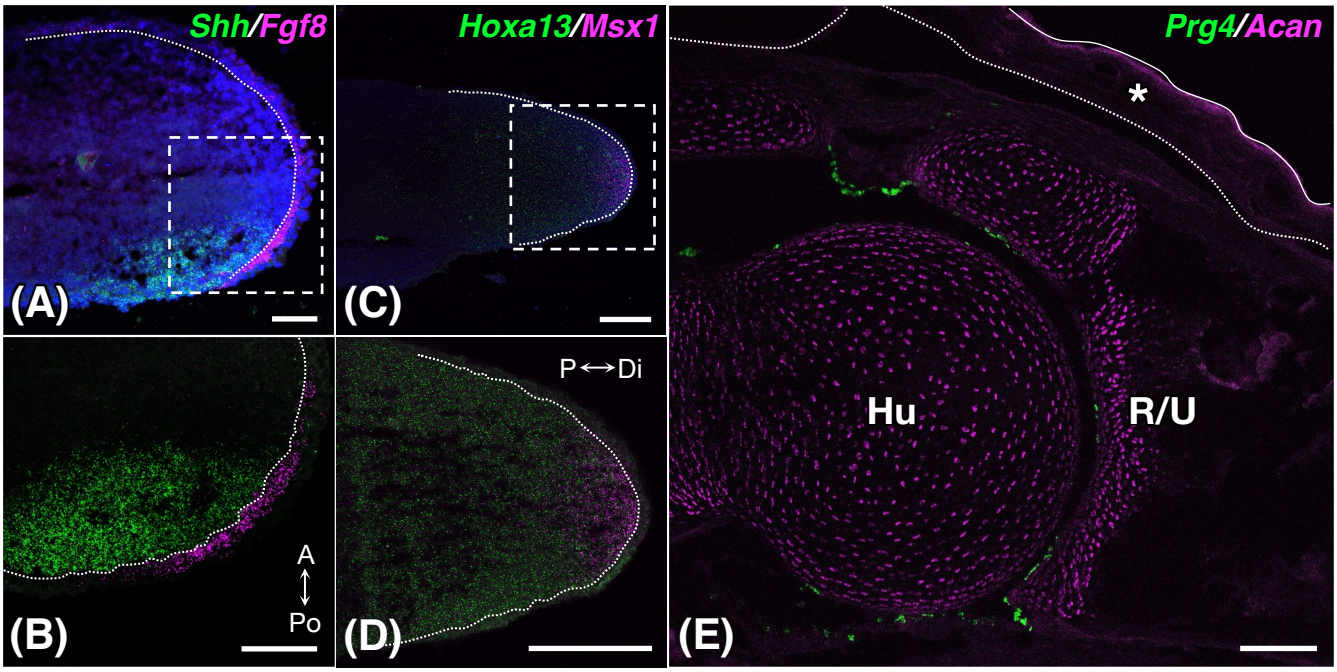


Fig.4

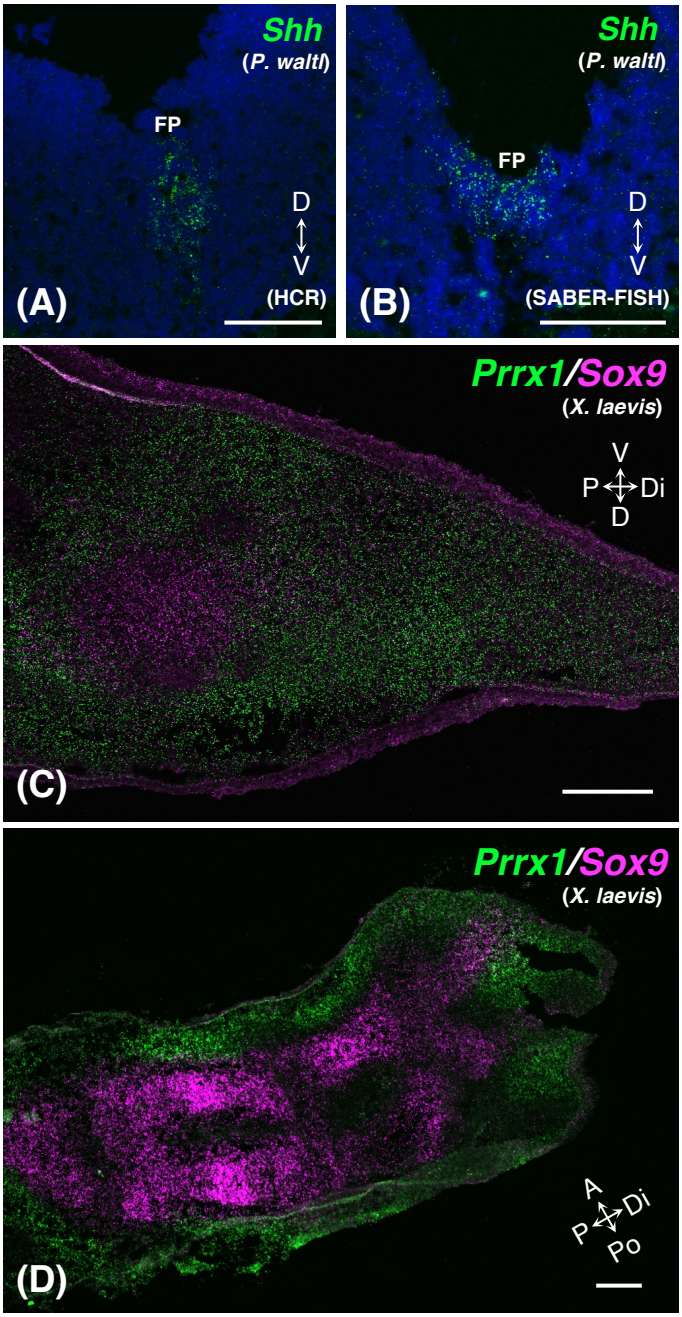
Shh
(P. waltl)
FP
D
V
(HCR)
(A)
Shh
(P. waltl)
FP
D
V
(SABER-FISH)
(B)
Prrx1/Sox9
(X. laevis)
V
P
Di
D
(C)
Prrx1/Sox9
(X. laevis)
A
P
Di
Po
(D)

Fig.5

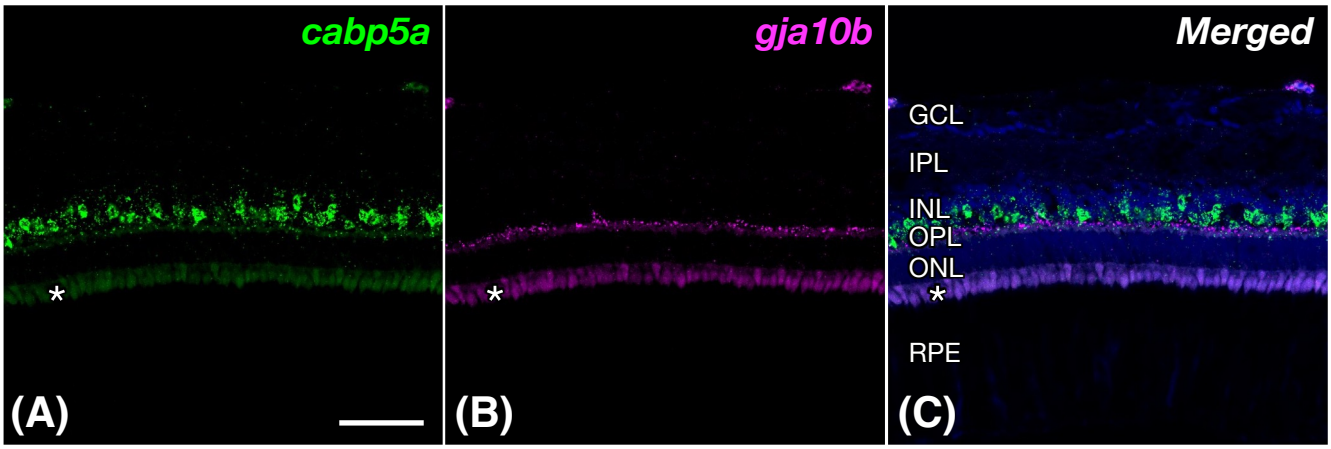


Fig.6